

# Multi-band magnetotransport in exfoliated thin films of $\text{Cu}_x\text{Bi}_2\text{Se}_3$

J.A. Alexander-Webber,<sup>1,\*</sup> J. Huang,<sup>2</sup> J. Beilsten-Edmands,<sup>2</sup>  
P. Čermák,<sup>3</sup> Č. Drašar,<sup>3</sup> R.J. Nicholas,<sup>2</sup> and A.I. Coldea<sup>2,†</sup>

<sup>1</sup>*Department of Engineering, University of Cambridge,  
J.J. Thomson Avenue, Cambridge CB3 0FA, United Kingdom*

<sup>2</sup>*Dept. of Physics, University of Oxford, Clarendon Laboratory, Parks Rd., Oxford, OX1 3PU, U.K.*

<sup>3</sup>*Faculty of Chemical Technology, University of Pardubice,  
Studentsk 573, 532 10 Pardubice, Czech Republic*

(Dated: February 14, 2018)

We report magnetotransport studies in thin ( $< 100\text{ nm}$ ) exfoliated films of  $\text{Cu}_x\text{Bi}_2\text{Se}_3$  and we detect an unusual electronic transition at low temperatures. Bulk crystals show weak superconductivity with  $T_c \sim 3.5\text{ K}$  and a possible electronic phase transition around  $200\text{ K}$ . Following exfoliation, superconductivity is suppressed and a strongly temperature dependent multi-band conductivity is observed for  $T < 30\text{ K}$ . This transition between competing conducting channels may be enhanced due to the presence of electronic ordering, and could be affected by the presence of an effective internal stress due to Cu intercalation. By fitting to the weak antilocalisation conductivity correction at low magnetic fields we confirm that the low temperature regime maintains a quantum phase coherence length  $L_\phi > 100\text{ nm}$  indicating the presence of topologically protected surface states.

Following the isolation of graphene by mechanical exfoliation<sup>1,2</sup> the properties of a great number of atomically thin Van der Waals crystals have gained considerable interest<sup>3,4</sup>. These two-dimensional materials occupy a wide spectrum of electronic properties from insulators to semiconductors and superconductors, and many of which vary dramatically from the properties of the bulk crystals when approaching the two-dimensional limit. Among this diverse class of materials a number of them, such as  $\text{Bi}_2\text{Se}_3$  and  $\text{Bi}_2\text{Te}_3$ , have been experimentally shown to behave as topological insulators<sup>5,6</sup>, bulk insulators with topologically protected metallic surface states of Dirac fermions<sup>7</sup>. In addition to their potential applications in electronics and spintronics, one of the key fundamental interests is to experimentally realise the quasi-particle excitations which behave as Majorana fermions<sup>8</sup> which are predicted to exist in the surface states of a topological insulator with induced superconductivity<sup>9</sup>. When doped with copper, bulk crystals of  $\text{Cu}_x\text{Bi}_2\text{Se}_3$  have been shown to undergo a superconducting phase transition with a  $T_c$  of up to  $3.8\text{ K}$ <sup>10–14</sup>, and are a possible candidate material for topological superconducting surface states hosting Majorana fermions. Critically angle resolved photoemission spectroscopy (ARPES) measurements have shown that even in the heavy doping regime ( $x = 0.25$ ) the Dirac surface states remain robust against dopants and impurities<sup>11,15</sup>.

$\text{Bi}_2\text{Se}_3$  is composed of quintuple layers of Se-Bi-Se-Bi-Se coupled by weak van der Waals bonding to the next quintuple layer. This van der Waals stacking means that in addition to easy basal plane cleavage for high quality mechanically exfoliated thin films, chemical doping of  $\text{Bi}_2\text{Se}_3$  is possible by both substitution and through intercalation<sup>10</sup>. Early experiments<sup>16</sup> showed that Cu dopants in  $\text{Bi}_2\text{Se}_3$  are ambipolar in nature acting as an electron donor through Cu-intercalation between the quintuple layers in  $\text{Cu}_x\text{Bi}_2\text{Se}_3$  and as an electron acceptor via Cu-substitution of Bi ( $\text{Bi}_{2-x}\text{Cu}_x\text{Se}_3$ ). How-

ever, while growth processes can be tuned to favour either intercalation or substitution<sup>10</sup>, the precise nature of Cu dopants in  $\text{Bi}_2\text{Se}_3$  remains controversial particularly given the apparent low doping efficiency and the observed saturation of the carrier density at high levels of doping ( $x > 0.1$ )<sup>15</sup>. This is further complicated by the apparent strong dependence of the device characteristics on growth and preparation technique<sup>17–20</sup>. This has led to speculation over the roles that the distribution<sup>18,19</sup> and valence states<sup>20</sup> of Cu dopant atoms within the lattice have in determining temperature dependent carrier transport and electronic ordering. In this Paper we observe a stark contrast between the electronic properties of  $\text{Cu}_{0.2}\text{Bi}_2\text{Se}_3$  in bulk crystals and those of mechanically exfoliated thin films derived from the same sample, where a new strongly temperature dependent conductivity is observed in the two-dimensional samples at temperatures below  $\sim 30\text{ K}$ . We attribute this to the presence of two competing parallel conduction channels, which may originate from the topological surface state ( $T < 30\text{ K}$ ) and the quantum confined two dimensional electron gas (2DEG) surface accumulation layer ( $T > 30\text{ K}$ ).

Crystals of  $\text{Cu}_{0.2}\text{Bi}_2\text{Se}_3$  were grown using a melt growth technique. Initial characterisation of the temperature dependent resistivity of bulk crystals,  $1\text{ mm}$  long with a thickness of  $\sim 50\text{ }\mu\text{m}$ , shows a weakly superconducting behaviour with a critical temperature of  $3.5\text{ K}$  (Fig. 1a) and a critical magnetic field of  $B_c < 1\text{ T}$ , which are both in good agreement with previous studies<sup>10,17</sup>. Thin films were cleaved from the sample surface using the “scotch tape technique” and deposited on a Si substrate with  $300\text{ nm}$  of thermally grown  $\text{SiO}_2$ . Au contacts were made to individual crystals by thermal deposition following electron-beam lithography. Two devices were studied in detail, Sample A, an  $80 \times 10\text{ }\mu\text{m}^2$  four terminal device and Sample B, a  $10 \times 10\text{ }\mu\text{m}^2$  Hall bar device. AFM characterisation reveals that the devices are approximately  $100\text{ nm}$  thick, above the thickness required

for topological effects<sup>21</sup> and three orders of magnitude less than the bulk crystal thickness. Low temperature four-terminal DC measurements were taken using Keithley DMM in a Helium flow variable temperature insert with a base temperature of 1.4 K. High magnetic fields were provided by an Oxford Instruments superconducting solenoid magnet.

Figure 1 is a comparison between the temperature dependent resistivity of bulk crystals and exfoliated thin films. As a function of temperature the resistivity of the bulk crystal exhibits a metallic behaviour before it becomes weakly superconducting at temperatures below 3.5 K. The superconducting phase is incomplete with a relatively large residual resistivity ratio which we attribute to inhomogeneous Cu doping. Upon the application of a magnetic field a critical field of  $B_c \sim 0.5$  T is observed at 2 K. Possible signatures of a higher temperature transition are observed at  $T_P^{Bulk} \sim 200$  K as highlighted in Figure 1a. The temperature dependence of the two-dimensional resistivity ( $\rho_{xx}$ ) in the exfoliated

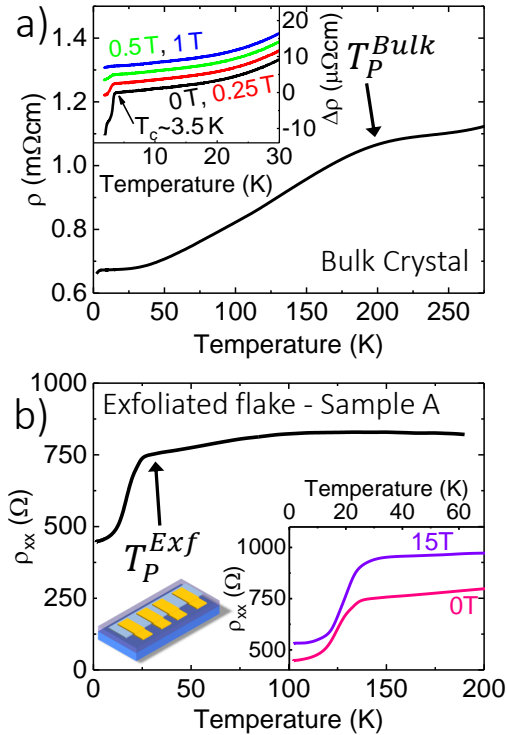


FIG. 1: a) Temperature dependent resistivity of bulk  $\text{Cu}_{0.2}\text{Bi}_2\text{Se}_3$  showing metallic behaviour until a critical temperature of  $T_c = 3.5$  K it undergoes a weak superconducting transition. Inset: Offset change in resistivity  $\Delta\rho$  at 0, 0.25, 0.5 and 1 T showing superconductivity with a critical field at 2 K of  $\sim 0.5$  T. b) The temperature dependent resistance of Sample A (shown schematically) at  $B = 0$  T is flat at higher temperatures and shows a significant drop in resistance below  $T_P^{Exf} \sim 30$  K. Inset: At high magnetic field the resistance continues to be strongly temperature dependent.

Sample A at 0 T is shown in Figure 1b. At high temperatures we observe a flat resistivity almost independent of temperature. When the sample is cooled below  $T_P^{Exf} \sim 30$  K  $\rho_{xx}$  significantly drops. Unlike the weak superconductivity observed in the bulk samples even the application of a 15 T magnetic field, does not suppress the strong temperature dependence (Fig. 1b inset). This behaviour is comparable to that observed recently in polycrystalline  $\text{Cu}_x\text{Bi}_2\text{Se}_3$  films<sup>20</sup>. It is also worth noting that there is a significant magneto-resistance in the high temperatures phase which is indicative of a higher mobility system<sup>22</sup>, as discussed below. Figure 2b shows that Sample B also exhibits a similar temperature dependence at  $T_P^{Exf} \sim 30$  K which is accompanied by a reduction in the magneto-resistance. It is clear that these samples undergo a significant change in their electronic properties at low temperatures and we must therefore investigate the temperature dependence of further electronic properties such as mobility and carrier density to elucidate the nature of this effect.

The temperature dependence of the Hall resistivity ( $\rho_{xy}$ ) of Sample B is shown in Figure 2a. We observe a substantial change in the Hall coefficient ( $\rho_{xy}/B$ ) through the transitional temperature regime indicating that a large number of additional carriers are present at low temperatures. In addition to the temperature dependent carrier density, the symmetrised  $\rho_{xy}$  values are non-linear in field. This is particularly clear in the vicinity of the transition as highlighted in Figure 2a. This non-linearity is indicative of a system with multiple carriers<sup>22</sup>. We model the system with two carriers with a carrier density of  $n_1$  and  $n_2$  with mobilities  $\mu_1$  and  $\mu_2$  respectively. The Hall resistivity is given by

$$\rho_{xy} = \frac{\sigma_{xy}}{\sigma_{xx}^2 + \sigma_{xy}^2}, \quad (1)$$

where the conductivities  $\sigma_{xx}$  and  $\sigma_{xy}$  as a function of magnetic field  $B$  are given by

$$\sigma_{xy} = \frac{n_1\mu_1^2B}{1+B^2\mu_1^2} + \frac{n_2\mu_2^2B}{1+B^2\mu_2^2}, \quad (2)$$

and

$$\sigma_{xx} = \frac{n_1\mu_1}{1+B^2\mu_1^2} + \frac{n_2\mu_2}{1+B^2\mu_2^2}. \quad (3)$$

The results of the two-carrier analysis are summarised in Figure 2c and d. In the high temperature phase we observe a single high mobility ( $\mu_1[50 \text{ K}] \sim 8000 \text{ cm}^2\text{V}^{-1}\text{s}^{-1}$ ) carrier with a density  $n_1 = 1.4 \times 10^{13} \text{ cm}^{-2}$ . It is worth noting that this corresponds to a three dimensional carrier density of  $n_1 \sim 3 \times 10^{18} \text{ cm}^{-3}$  and is significantly lower than the carrier density of the bulk samples which were measured to have  $n_{bulk} = 3 \times 10^{19} \text{ cm}^{-3}$ . This is of particular importance in explaining the lack of superconductivity in the exfoliated samples as typically much

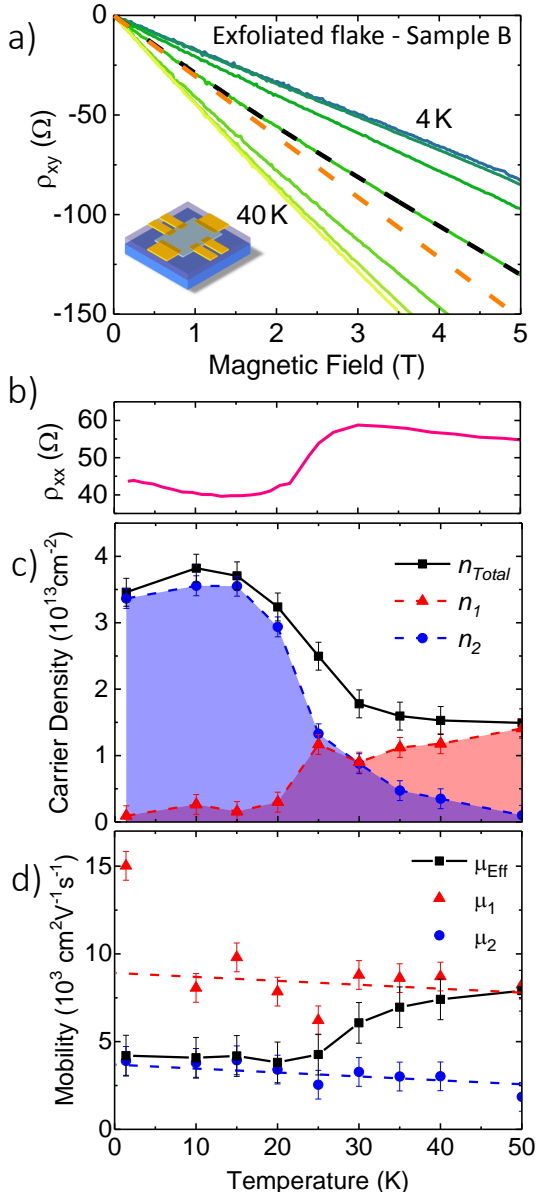


FIG. 2: a) Magnetic field dependence of the symmetrised Hall resistance,  $\rho_{xy}$ , in the transitional temperature region for sample B (shown schematically), exhibiting predominantly electron-like behaviour. The dashed orange and black lines are an extrapolation of  $\rho_{xy}$  from low fields and a fit to Equation 1 respectively for the trace at 25 K. This demonstrates that the field dependence of the Hall coefficient is characteristic of a two-carrier system. b) Temperature dependence of  $\rho_{xx}$  at  $B = 0$  T. c) Results of two-carrier analysis from Equation 1 showing the temperature dependence of respective carrier densities  $n_1$  (red), dominant at high temperatures, and  $n_2$  (blue) which increases significantly at low temperatures. The total carrier density ( $n_{Total}$ , black) more than doubles at low temperatures indicating a significant change in the relative contributions of the two parallel conduction channels. d) The temperature dependent mobility  $\mu_1$  (red) and  $\mu_2$  (blue) of carriers  $n_1$  and  $n_2$  respectively. Also shown is the effective mobility (black) where  $\mu_{Eff}^{-1} = n_{Total} e \rho_{xx}$ . Dashed lines are guides to the eye.

higher carrier densities are required<sup>12</sup>. This could be an indication that nonuniformity of Cu intercalation during the doping process results in areas or clusters of lower doping and the exfoliated flakes represent a region of low doping. Similarly, it is known that Cu atoms may diffuse towards the surface when exposed to air. Whilst the samples were stored and measured under vacuum, air exposure would have occurred during sample preparation and lithography. As the temperature is reduced an additional low mobility ( $\mu_2 \sim 3400 \text{ cm}^2 \text{ V}^{-1} \text{ s}^{-1}$ ) carrier  $n_2$  appears and increases in density. Between 25 K and 30 K, corresponding to the same temperature at which the first signatures of the transition are observed in the zero field resistivity, the two carriers contribute approximately equally to the total carrier density. Then at low temperatures  $n_2$  continues to increase to a maximum value of  $n_2 = 3.5 \times 10^{13} \text{ cm}^{-2}$  completely replacing  $n_1$  and dominating the conduction of the low temperature regime, further indication that there may be a significant modification of the electronic bands in exfoliated  $\text{Cu}_{0.2}\text{Bi}_2\text{Se}_3$ .

Previous two-carrier Hall effect measurements of  $\text{Bi}_2\text{Se}_3$  films have revealed the presence of two coexisting surface conduction channels<sup>23,24</sup>. A high density ( $3 \times 10^{13} \text{ cm}^{-2}$ ), lower mobility ( $\sim 500 \text{ cm}^2 \text{ V}^{-1} \text{ s}^{-1}$ , due to increased surface scattering<sup>24</sup>) state which was determined to originate from the topological surface state, and a lower density ( $8 \times 10^{12} \text{ cm}^{-2}$ ), higher mobility ( $3000 \text{ cm}^2 \text{ V}^{-1} \text{ s}^{-1}$ ) state which was determined to originate from a quantum confined 2DEG accumulation layer formed due to surface band bending<sup>25</sup>. The respective origins of each of the two states can be determined from thickness dependent measurements<sup>23</sup>. The distinction can be made because if the total thickness of the sample is reduced to less than twice the depth of the surface accumulation layer ( $\lesssim 8 \text{ nm}$ ), the lowest lying energy bands of the 2DEG are raised above the Fermi level due to quantum confinement<sup>23</sup> and are no longer populated. The surface accumulation 2DEG is a parabolic band with a similar energy to the bulk conduction band<sup>26,27</sup> and has been calculated to strongly depend on the thickness of the van der Waals gap which in turn is determined by the presence of intercalants, either intentional such as in  $\text{Cu}_x\text{Bi}_2\text{Se}_3$  or unintentionally due to air exposure<sup>28</sup>. The qualitative descriptions of the two bands are consistent with the results of our two-carrier fitting shown above. For undoped  $\text{Bi}_2\text{Se}_3$  these two states can coexist at low temperatures. For  $\text{Cu}_x\text{Bi}_2\text{Se}_3$  we see that a transitional regime of competing channels occurs for  $T < 30 \text{ K}$ . A comparison of our results with these reports suggests that at temperatures above  $T_P^{Exf}$  transport in our exfoliated  $\text{Cu}_x\text{Bi}_2\text{Se}_3$  samples is dominated by the surface accumulation 2DEG layer. As the temperature is decreased through a coexistence regime the low temperature transport may then be dominated by topological surface states. Another possible origin of this transition is the presence of impurity bands<sup>29–31</sup> which have been shown in  $\text{Bi}_2\text{Se}_3$  at temperatures below 40 K to cause a

small ( $< 10\%$ ) increase in the measured carrier density due to thermally activated conductivity<sup>30,31</sup>. If this were the case in our samples, due to the magnitude of the effect, it would require that impurity band transport is dominant at low temperatures. However, the presence of weak antilocalisation (WAL), described below, suggests that coherent transport is maintained in our samples which may indicate that a topological origin of the low temperature transport is more likely.

In undoped  $\text{Bi}_2\text{Se}_3$ , band structure modifications and resulting non-trivial temperature dependences are commonly observed due to applied strain<sup>32,33</sup> and pressure<sup>34,35</sup>. Indeed, in single crystals of undoped  $\text{Bi}_2\text{Se}_3$  at applied pressures of between 5 to 6 GPa, i.e. below the pressure required to induce superconductivity ( $\sim 12$  GPa), Kong *et al.*<sup>34</sup> observe a temperature dependent resistivity which is visually similar to those we observe. Such observations may not at first appear directly relevant to the results presented here which were obtained in the absence of externally applied pressure or strain. However, by comparing ARPES measurements with *ab initio* band structure calculations, it has been shown that when compared to undoped  $\text{Bi}_2\text{Se}_3$  the effect of Cu intercalation on the band structure is equivalent to that calculated under several GPa of uniaxial pressure<sup>36</sup>. Thus, our observations may be due to a combination of an *effective* internal stress at doping levels insufficient to observe the superconducting phase but which may allow enhanced electron correlation effects to drive the observed sharp transition between the two conductive channels. Such electronic ordering effects are common in a number of layered compounds at low temperatures affecting many properties including resistivity, carrier density and magnetic susceptibility<sup>37–39</sup>. Intercalation has been shown to significantly alter electronic correlation effects in layered compounds. For example, by varying the Cu concentration in  $\text{Cu}_x\text{TiSe}_2$  the dominant electronic ordering can be varied from a charge density wave state at low doping to superconductivity at higher Cu concentration<sup>40</sup>. It is conceivable that the Cu intercalation in  $\text{Cu}_x\text{Bi}_2\text{Se}_3$  alters the electronic ordering which in bulk samples enables superconductivity and in exfoliated samples drives the strongly temperature dependent multi-band transport that we observe here.

A common feature of the transport properties of topological insulators is the presence of weak anti localisation (WAL), a positive correction to the conductivity due to destructive quantum interference between scattering loops during diffusive transport<sup>41</sup>.  $\text{Cu}_x\text{Bi}_2\text{Se}_3$  also shows clear WAL properties allowing us to probe the coherent properties of the electronic transport. Hikami *et al.*<sup>42</sup> predict that a topological insulator is expected to exhibit WAL described by the equation

$$\Delta\sigma(B) = \alpha \frac{e^2}{\pi h} \left[ \ln \frac{B_0}{B} - \psi \left( \frac{1}{2} + \frac{B_0}{B} \right) \right], \quad (4)$$

where  $B_0 = \hbar/4De\tau_\phi$ ,  $\tau_\phi$  being the phase coherence

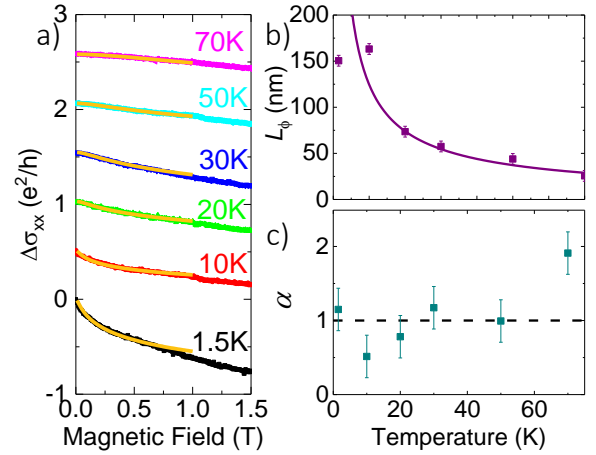


FIG. 3: a) Change in symmetrised conductivity  $\Delta\sigma_{xx} = \sigma_{xx}(B) - \sigma_{xx}(0)$  of Sample A as a function of magnetic field  $B$  showing clear signatures of weak antilocalisation and WAL fits using Equation 4 (orange). Traces are vertically offset for clarity. We extract b) scattering length  $L_\phi$ , which is fitted by  $T^{-3/4}$ , and c)  $\alpha$  which is a measure of the number of 2D electronic channels contributing to the WAL where  $\alpha = 1$  (black dashed) corresponds to two coherent channels.

time and the diffusion constant  $D = v_F^2/2\tau_{tr}$  which is given by the Fermi velocity<sup>5</sup>  $v_F \sim 5 \times 10^5 \text{ ms}^{-1}$  and the transport scattering time  $\tau_{tr}$  ( $\sim 250 \text{ fs}$  for  $3500 \text{ cm}^2\text{V}^{-1}\text{s}^{-1}$ ), and where  $\psi$  is the digamma function and  $\alpha$  is the amplitude of the correction. It is predicted<sup>42</sup> that  $\alpha$  is related to the number of conducting channels which contribute to the WAL effect and takes a value of  $\alpha = 1/2$  per channel. Figure 3 shows the change in low field conductivity  $\Delta\sigma_{xx}$  of Sample A at relatively low magnetic fields from  $T = 1.5 \text{ K}$  to  $70 \text{ K}$ . We find that Equation 4 describes the low field conductivity very well as shown in Figure 3a. From these fits we can extract the temperature dependence of the coherence length  $L_\phi = \sqrt{D\tau_\phi}$  and  $\alpha$  shown in Figure 3b and c. At low temperature we find a maximum value of  $L_\phi^{max} \sim 160 \text{ nm}$  which corresponds to a dephasing time of  $\tau_\phi^{max} \sim 1 \text{ ps}$ . The phase coherence length increases as the temperature is reduced following a  $L_\phi \propto T^{-p/2}$  where  $p = 1.5$  indicating that the low temperature phase retains the quantum coherence of the topologically protected surface states<sup>43</sup>. We find a relatively constant value of  $\alpha \sim 1$  which corresponds to two decoupled phase coherent channels. We attribute this to the two parallel conduction channels discussed above.

In conclusion we have used magnetotransport measurements to observe a strongly temperature dependent conductivity in exfoliated thin films of  $\text{Cu}_x\text{Bi}_2\text{Se}_3$ . The transitional temperature regime of  $\sim 30 \text{ K}$  is not observed in bulk samples prior to exfoliation. The high temperature regime is characterised by a low density but high mobility carrier which is replaced at low temperatures by a



higher density carrier which greatly enhances the overall carrier density of the devices thus significantly reducing the overall resistance. This transition between competing conducting channels may be enhanced due to the presence of electronic ordering, and could be affected by the presence of an effective internal stress due to Cu intercalation. Based on previous two-carrier magnetotransport measurements of undoped  $\text{Bi}_2\text{Se}_3$  these results are consistent with a high temperature regime where transport is dominated by a surface accumulation 2DEG state which transitions to low temperature transport dominated by a topological surface state. At low temperatures through fitting the WAL conductivity peak we find long quantum coherence lengths indicative of decoupled surface states. We believe these results are important in understanding

the interplay between the surface states and superconductivity in  $\text{Cu}_x\text{Bi}_2\text{Se}_3$  as well as new types of competing electronic order in this class of materials.

## I. ACKNOWLEDGEMENTS

This work was supported by EPSRC (EP/L001772/1, EP/I004475/1, EP/I017836/1). AIC acknowledges an EPSRC Career Acceleration Fellowship (EP/I004475/1). JAA-W acknowledges the support of his Research Fellowship from the Royal Commission for the Exhibition of 1851.

\* Electronic address: [jaa59@cam.ac.uk](mailto:jaa59@cam.ac.uk)

† Electronic address: [amalia.coldea@physics.ox.ac.uk](mailto:amalia.coldea@physics.ox.ac.uk)

- <sup>1</sup> K. S. Novoselov, A. K. Geim, S. V. Morozov, D. Jiang, M. I. Katsnelson, I. V. Grigorieva, S. V. Dubonos, and A. A. Firsov, *Nature* **438**, 197 (2005).
- <sup>2</sup> Y. Zhang, Y.-W. Tan, H. L. Stormer, and P. Kim, *Nature* **438**, 201 (2005).
- <sup>3</sup> K. S. Novoselov, D. Jiang, F. Schedin, T. J. Booth, V. V. Khotkevich, S. V. Morozov, and A. K. Geim, *Proceedings of the National Academy of Sciences of the United States of America* **102**, 10451 (2005).
- <sup>4</sup> A. H. C. Neto and K. S. Novoselov, *Reports on Progress in Physics* **74**, 082501 (2011).
- <sup>5</sup> H. Zhang, C.-X. Liu, X.-L. Qi, X. Dai, Z. Fang, and S.-C. Zhang, *Nature Physics* **5**, 438 (2009).
- <sup>6</sup> Y. L. Chen, J. G. Analytis, J.-H. Chu, Z. K. Liu, S.-K. Mo, X. L. Qi, H. J. Zhang, D. H. Lu, X. Dai, Z. Fang, S. C. Zhang, I. R. Fisher, Z. Hussain, Z. X. Shen, *Science* **325**, 178 (2009).
- <sup>7</sup> M. Z. Hasan and C. L. Kane, *Reviews of Modern Physics* **82**, 3045 (2010).
- <sup>8</sup> F. Wilczek, *Nature Physics* **5**, 614 (2009).
- <sup>9</sup> L. Fu and C. Kane, *Physical Review Letters* **100**, 096407 (2008).
- <sup>10</sup> Y. S. Hor, A. J. Williams, J. G. Checkelsky, P. Roushan, J. Seo, Q. Xu, H. W. Zandbergen, A. Yazdani, N. P. Ong, and R. J. Cava, *Physical Review Letters* **104**, 057001 (2010).
- <sup>11</sup> L. A. Wray, S.-Y. Xu, Y. Xia, Y. S. Hor, D. Qian, A. V. Fedorov, H. Lin, A. Bansil, R. J. Cava, and M. Z. Hasan, *Nature Physics* **6**, 855 (2010).
- <sup>12</sup> M. Kriener, K. Segawa, Z. Ren, S. Sasaki, and Y. Ando, *Physical Review Letters* **106**, 127004 (2011).
- <sup>13</sup> S. Sasaki, M. Kriener, K. Segawa, K. Yada, Y. Tanaka, M. Sato, and Y. Ando, *Physical Review Letters* **107**, 217001 (2011).
- <sup>14</sup> K. Matano, M. Kriener, K. Segawa, Y. Ando, and G. Zheng, *Nat. Phys.* **12**, 852 (2016).
- <sup>15</sup> Y. Tanaka, K. Nakayama, S. Souma, T. Sato, N. Xu, P. Zhang, P. Richard, H. Ding, Y. Suzuki, P. Das, K. Kad-owaki, and T. Takahashi, *Physical Review B* **85**, 125111 (2012).
- <sup>16</sup> A. Vaško, L. Tichý, J. Horák, and J. Weissenstein, *Applied Physics* **5**, 217 (1974).
- <sup>17</sup> M. Kriener, K. Segawa, Z. Ren, S. Sasaki, S. Wada, S. Kuwabata, and Y. Ando, *Physical Review B* **84**, 054513 (2011).
- <sup>18</sup> T. Shirasawa, M. Sugiki, T. Hirahara, M. Aitani, T. Shirai, S. Hasegawa, and T. Takahashi, *Phys. Rev. B* **89**, 195311 (2014).
- <sup>19</sup> M. Wang, Y. Song, L. You, Z. Li, B. Gao, X. Xie, and M. Jiang, *Sci. Rep.* **6**, 22713 (2016).
- <sup>20</sup> M. Li, Z. Wang, L. Yang, D. Li, Q.R. Yao, G.H. Rao, X.P.A. Gao, and Z. Zhang, *Phys. Rev. B* **96**, 75152 (2017).
- <sup>21</sup> Y. Zhang, K. He, C.-Z. Chang, C.-L. Song, L.-L. Wang, X. Chen, J.-F. Jia, Z. Fang, X. Dai, W.-Y. Shan, S.-Q. Shen, Q. Niu, X.-L. Qi, S.-C. Zhang, X.-C. Ma, and Q.-K. Xue, *Nature Physics* **6**, 584 (2010).
- <sup>22</sup> N. W. Ashcroft and N. D. Mermin, *Solid State Physics* (Saunders College, Philadelphia, 1976).
- <sup>23</sup> N. Bansal, Y. S. Kim, M. Brahlek, E. Edrey, and S. Oh, *Phys. Rev. Lett.* **109**, 116804 (2012).
- <sup>24</sup> E.K. de Vries, S. Pezzini, M.J. Meijer, N. Koirala, M. Salehi, J. Moon, S. Oh, S. Wiedmann, and T. Banerjee, *Phys. Rev. B* **96**, 45433 (2017).
- <sup>25</sup> M. Brahlek, N. Koirala, N. Bansal, and S. Oh, *Solid State Commun.* **54**, 215216 (2015).
- <sup>26</sup> M. Bianchi, D. Guan, S. Bao, J. Mi, B.B. Iversen, P.D.C. King, and P. Hofmann, *Nat. Commun.* **1**, 128 (2010).
- <sup>27</sup> M. S. Bahrany, P. D. King, A. de la Torre, J. Chang, M. Shi, L. Patthey, G. Balakrishnan, P. Hofmann, R. Arita, N. Nagaosa, and F. Baumberger, *Nat. Commun.* **3**, 1159 (2012).
- <sup>28</sup> T. V. Menshchikova, S. V. Eremeev, and E. V. Chulkov, *JETP Lett.* **94**, 106 (2011).
- <sup>29</sup> V. Kulbachinskii, N. Miura, H. Nakagawa, H. Arimoto, T. Ikaida, P. Lostak, and C. Drašar, *Phys. Rev. B* **59**, 15733 (1999).
- <sup>30</sup> J.G. Analytis, J.H. Chu, Y. Chen, F. Corredor, R.D. McDonald, Z.X. Shen, and I.R. Fisher, *Phys. Rev. B* **81**, 205407 (2010).
- <sup>31</sup> S. Wiedmann, A. Jost, B. Fauqué, J. Van Dijk, M.J. Meijer, T. Khouri, S. Pezzini, S. Grauer, S. Schreyeck, C. Brüne, H. Buhmann, L.W. Molenkamp, and N.E. Hussey, *Phys. Rev. B* **94**, 081302 (2016).
- <sup>32</sup> Y. Liu, Y. Y. Li, S. Rajput, D. Gilks, L. Lari, P. L. Galindo, M. Weinert, V. K. Lazarov, and L. Li, *Nature Physics* **10**,

- 294 (2014).
- <sup>33</sup> T.-H. Kim, K. Jeong, B. C. Park, H. Choi, S. H. Park, S. Jung, J. Park, K.-H. Jeong, J. W. Kim, J. H. Kim, and M.-H. Cho, *Nanoscale* **8**, 741 (2015).
  - <sup>34</sup> P. P. Kong, J. L. Zhang, S. J. Zhang, J. Zhu, Q. Q. Liu, R. C. Yu, Z. Fang, C. Q. Jin, W. G. Yang, X. H. Yu, J. L. Zhu, and Y. S. Zhao, *J. Phys. Condens. Matter* **25**, 362204 (2013).
  - <sup>35</sup> K. Kirshenbaum, P. S. Syers, A. P. Hope, N. P. Butch, J. R. Jeffries, S. T. Weir, J. J. Hamlin, M. B. Maple, Y. K. Vohra, and J. Paglione, *Phys. Rev. Lett.* **111**, 087001 (2013).
  - <sup>36</sup> A. Ribak, K. B. Chashka, E. Lahoud, M. Naamneh, S. Rinott, Y. Ein-Eli, N. C. Plumb, M. Shi, E. Rienks, and A. Kanigel, *Physical Review B* **93**, 064505 (2016).
  - <sup>37</sup> J. Wilson, F. D. Salvo, and S. Mahajan, *Physical Review Letters* **32**, 882 (1974).
  - <sup>38</sup> D. E. Moncton, J. D. Axe, and F. J. DiSalvo, *Phys. Rev. B* **16**, 801 (1977).
  - <sup>39</sup> J. A. Wilson, F. J. Di Salvo, and S. Mahajan, *Advances in Physics* **24**, 117 (1975).
  - <sup>40</sup> E. Morosan, H.W. Zandbergen, B.S. Dennis, J.W.G. Bos, Y. Onose, T. Klimczuk, A.P. Ramirez, N.P. Ong, and R.J. Cava, *Nat. Phys.* **2**, 544 (2006).
  - <sup>41</sup> Y. Takagaki, B. Jenichen, U. Jahn, M. Ramsteiner, and K.-J. Friedland, *Phys. Rev. B* **85**, 115314 (2012).
  - <sup>42</sup> S. Hikami, A. Larkin, and Y. Nagaoka, *Progress of Theoretical Physics* **63**, 707 (1980).
  - <sup>43</sup> P. A. Lee, and T. V. Ramakrishnan, *Rev. Mod. Phys.* **57**, 287337 (1985).
  - <sup>44</sup> D. Kim, P. Syers, N. P. Butch, J. Paglione, and M. S. Fuhrer, *Nature communications* **4**, 2040 (2013).
  - <sup>45</sup> H. Steinberg, J.-B. Laloë, V. Fatemi, J. S. Moodera, and P. Jarillo-Herrero, *Physical Review B* **84**, 233101 (2011).